



## Organic electroluminescence devices based on anthracene sulfide derivatives

Chakkrapan Nerungsi<sup>a</sup>, Piangkhan Wanitchang<sup>b</sup>, Somboon Sahasithiwat<sup>c</sup>, Karoon Sadorn<sup>a</sup>,  
Teerakiat Kerdcharoen<sup>b</sup>, Tienthong Thongpanchang<sup>a,d,\*</sup>

<sup>a</sup> Department of Chemistry and Center of Excellence for Innovation in Chemistry, Faculty of Science, Mahidol University, Rama 6 Road, Bangkok 10400, Thailand

<sup>b</sup> Department of Physics, Faculty of Science, Mahidol University, Rama 6 Road, Bangkok 10400, Thailand

<sup>c</sup> National Metal and Materials Technology Center, National Science and Technology Development Agency, Thailand Science Park, Phatumthani 12120, Thailand

<sup>d</sup> National Center for Genetic Engineering and Biotechnology, National Science and Technology Development Agency, Thailand Science Park, Phatumthani 12120, Thailand

### ARTICLE INFO

#### Article history:

Received 10 April 2010

Revised 25 August 2010

Accepted 20 September 2010

Available online 29 September 2010

### ABSTRACT

A series of anthracene derivatives are synthesized and fabricated as light-emitting materials in OLED devices. The incorporation of the chalcogen atoms, either oxygen or sulfur, in between the anthracene moiety and the alkyl or aryl substituents affected drastically the photo- and electroluminescence properties of the materials, especially the HOMO–LUMO band gap and the emitting color of the devices. The new anthracene sulfide derivatives represent a new design for further modification of other light-emitting doped materials.

© 2010 Elsevier Ltd. All rights reserved.

### 1. Introduction

Small organic molecules that exhibit red,<sup>1</sup> green<sup>2</sup> or blue<sup>3</sup> colors have been widely investigated for the development of electronic devices such as organic light-emitting diodes (OLEDs). Among the blue emitters, anthracene derivatives demonstrate high-performance with excellent photoluminescence and electroluminescence properties.<sup>4</sup> Interestingly, recent reports indicated that introduction of heteroatoms, especially chalcogens, onto the anthracene core could change its molecular characteristics and electronic properties.<sup>5</sup> In this letter, anthracene sulfides, [9,10-bis(1-dodecylthio)anthracene (**ADS**), 9,10-bis(1-propylthio)anthracene (**APrS**), 9,10-bis(phenylthio)anthracene (**APS**), and 9,10-bis(2-naphthylthio)anthracene (**ANS**)] and an ether, [9,10-bis(1-dodecyloxy)anthracene (**ADO**)] were prepared and their properties as light emitting materials in OLED devices were investigated. **ADO** and **ADS** were designed to demonstrate the influence of the chalcogen atoms while **ADS**, **APrS**, **APS**, and **ANS** would highlight the effect of the type of alkyl or aryl side chains as well as the effect of chain length.

As shown in Scheme 1, 9,10-bis(1-dodecyloxy)anthracene (**ADO**) was prepared by the reduction of 9,10-anthraquinone (**1**) with Na<sub>2</sub>S<sub>2</sub>O<sub>4</sub>,<sup>6</sup> followed by Williamson ether synthesis in the presence of KOH and 1-bromododecane (34% overall yield). For the synthesis of anthracene sulfide derivatives, treatment of anthraquinone **1** with Zn, K<sub>2</sub>CO<sub>3</sub>, and acetic anhydride in THF provided 9,10-diacetoxyanthracene (**2**) in 87% yield. The acid-mediated substitution reaction of anthracene **2** with dodecane, propane, benzene, and 2-naphthalene thiols gave disulfide derivatives; **ADS**, **APrS**, **APS**, and **ANS** in 81%, 71%, 36%, and 17% yields, respectively.<sup>7,8</sup>

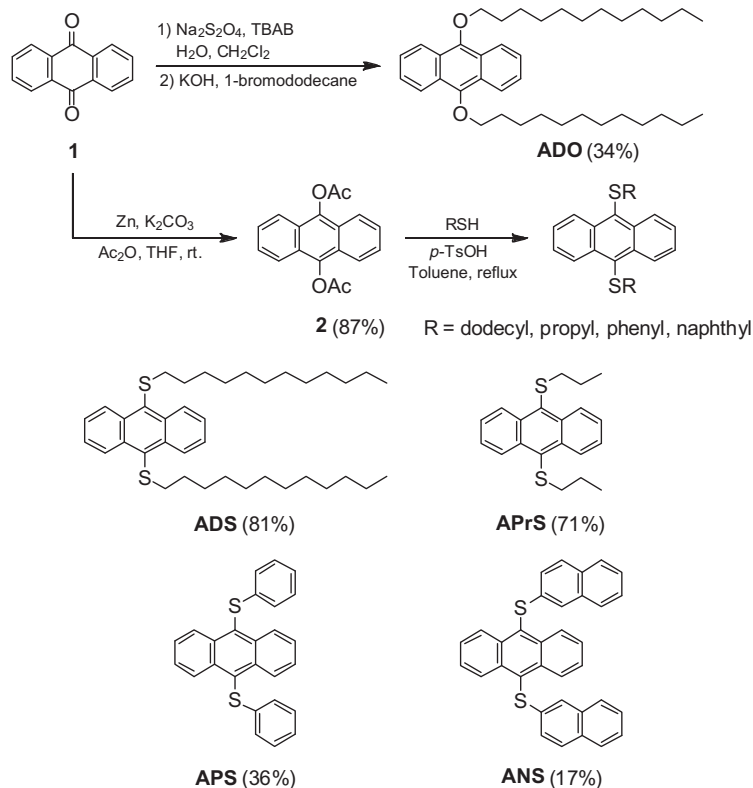
The UV absorption and fluorescence spectra of the anthracene derivatives were recorded in chloroform, Figure 1. All the absorption spectra exhibited similar characteristic vibrational patterns of the anthracene group in the region of 340–420 nm.<sup>4a</sup> The bathochromic shift (5 nm) of the sulfide derivative **ADS** in comparison to that of the ether derivative **ADO** indicated that the decrease in the HOMO–LUMO band gap (Fig. 2) was due to an electron delocalization effect from the heavier chalcogen atom.<sup>5</sup> Alkyl substituents with different chain lengths did not affect substantially the electronic properties of the anthracene as was evident from the indistinguishable spectra of **ADS** and **APrS**. In contrast, the aryl substituents, both phenyl (of **APS**) and naphthyl (of **ANS**), caused a red shift, possibly due to the participation of the conjugated system between the aryl substituents and the anthracene ring. The fluorescence spectra of anthracene derivatives show blue emission with a maximum peak at 442–476 nm. Similar to the absorption spectra, bathochromic shifts in the emission spectra were also observed upon changing the substituents.

The relative fluorescence quantum yields ( $\Phi_f$ ) of the anthracene derivatives in dilute CHCl<sub>3</sub> solution were measured using harmaline ( $\Phi_f \sim 0.83$ ) and harmine ( $\Phi_f \sim 0.45$ )<sup>9</sup> as calibration standards. All the anthracene sulfide derivatives gave fluorescence quantum yields of 0.006–0.048 whereas the ether derivative (**ADO**) gave a high fluorescence quantum yield of 0.46 (Table 1). The lower  $\Phi_f$  of the other anthracene sulfide derivatives might be attributed to quenching from the sulfide substituents, that is, the sulfur lone pair of electrons participated in the photo-induced electron transfer to the excited state of the anthracene.<sup>10</sup>

The effect of a sulfur atom on the photo- and electrochemical properties of the anthracene core could be substantiated by comparison of the UV and fluorescence spectra as well as the HOMO–LUMO band gap between **ANS** and the non-sulfur

\* Corresponding author. Tel./fax: +66 2 201 5139.

E-mail address: [tettp@mahidol.ac.th](mailto:tettp@mahidol.ac.th) (T. Thongpanchang).



Scheme 1. Syntheses of anthracene derivatives.

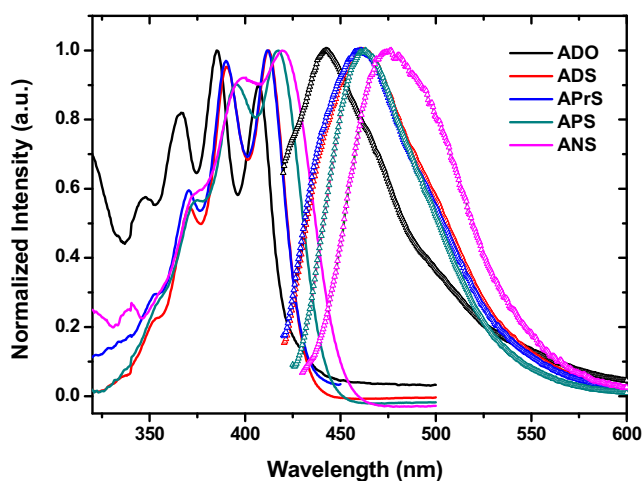
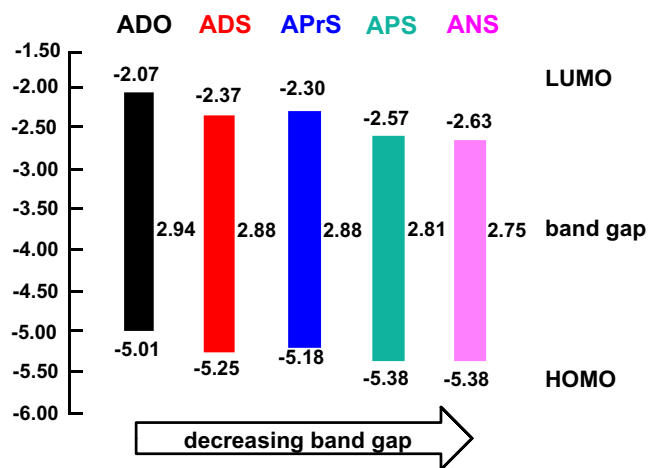
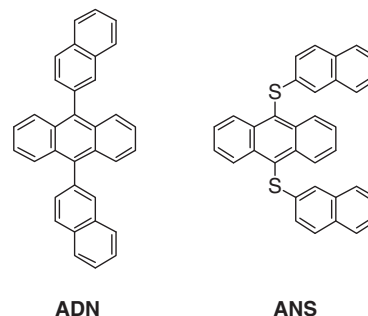
Figure 1. UV (—) and fluorescence spectra ( $\Delta$ ) of the anthracene derivatives.

Figure 2. The energy levels of the HOMO–LUMO orbitals of the anthracene derivatives.

derivative, 9,10-bis(2-naphthyl)anthracene (**ADN**).<sup>4a</sup> **ANS** showed a red shift of 42 nm in the UV spectrum, (from 377 nm in **ADN** to 419 nm in **ANS**), corresponding to a decrease in the band gap from 3.01 to 2.75 eV. The HOMO and LUMO energy levels of **ANS** (–5.38 and –2.63 eV, respectively) were higher than those of **ADN** (–5.88 and –2.87 eV, respectively). In addition, a red shift of 49 nm in the fluorescence spectrum of **ANS** ( $\lambda_{\text{em}}$  at 476 nm) compared to **ADN** ( $\lambda_{\text{em}}$  at 427 nm) was also observed. These results demonstrate the participation of the sulfur atom in the anthracene conjugated system, resulting in a drastic change in the electronic properties of the anthracene ring.



**Table 1**  
Physical data of anthracene derivatives and electroluminescence performances of their devices

Compound	$\lambda_{\text{max, abs}}^{\text{a}}$ (nm)	$\lambda_{\text{max, em}}^{\text{b}}$ (nm)	$T_{\text{m}}^{\text{c}}$ (°C)	$\Phi_{\text{f}}^{\text{d}}$	HOMO <sup>e</sup> /LUMO <sup>f</sup> (eV)	Turn-on voltage <sup>g</sup> (V)	$I_{\text{eff, max}}^{\text{g}}$ (cd/A)	$B_{\text{max}}^{\text{g}}$ at voltage		EL $\lambda_{\text{max}}^{\text{g}}$ (nm)	CIE (x, y) <sup>g</sup>
								(cd/m <sup>2</sup> )	(V)		
<b>ADO</b>	407	442	50	0.46	−5.01/−2.07	6.6	0.08	214	11.5	450	0.17, 0.14
<b>ADS</b>	412	460	69	0.048	−5.25/−2.37	6.9	0.09	319	10.5	465	0.16, 0.16
<b>APrS</b>	412	461	109	0.023	−5.18/−2.30	8.8	0.08	203	13.5	465	0.17, 0.17
<b>APS</b>	417	463	213	0.038	−5.38/−2.57	7.8	0.11	290	11.0	465	0.17, 0.18
<b>ANS</b>	419	476	239	0.006	−5.38/−2.63	8.6	0.03	132	11.0	470	0.20, 0.22

<sup>a</sup> Maximum absorption wavelength in CHCl<sub>3</sub>.

<sup>b</sup> Maximum emission wavelength in CHCl<sub>3</sub>.

<sup>c</sup> Obtained from differential scanning calorimetry (DSC) measurements.

<sup>d</sup> Fluorescence quantum yield in CHCl<sub>3</sub>.

<sup>e</sup> HOMO level was determined from the onset of the first oxidation wave in the cyclic voltammogram.

<sup>f</sup> LUMO level was calculated from the difference between the HOMO level and the optical band gap estimated from the onset of the lowest-energy visible absorption edge.

<sup>g</sup> Obtained from the electroluminescence devices.

The electroluminescence properties of **ADO**, **ADS**, **APrS**, **APS**, and **ANS** were investigated. All the synthetic materials were subjected to device fabrication in simple doped device structures (Fig. 3). Due to the low melting temperatures and potentially close  $\pi$ -stack solid state packing of **ADO**, **ADS**, and **APrS**,<sup>5,11</sup> poly(*N*-vinylcarbazole) (PVK) was used as a host material matrix in all the electroluminescence (EL) devices to improve the film-forming properties in the emitting layer, which was fabricated by a spin coating process.<sup>12</sup> Thus the OLED devices prepared in this work have the following structure: indium tin oxide (ITO) (*anode*)|3,4-polyethylene-dioxythiophene:polystyrene sulfonate (PEDOT:PSS) (35 nm) (*hole transporting layer*)|PVK:anthracene derivatives 1 wt % (68 nm) (*emitting layer*)|Ca (10 nm) (*cathode*)|Al (100 nm) (*protective layer*).

The current density–voltage and the luminance–voltage characteristics of the OLED devices are shown in Figures 3 and 4. The maximum EL brightness of **ADO**, **ADS**, **APrS**, **APS**, and **ANS** reached 214, 319, 203, 290, and 132 cd/m<sup>2</sup>, respectively. Figure 5 shows the plots of current efficiency versus current density of the devices. The **ADO**-based device exhibited a maximum current efficiency in the same range as those of the sulfur analogs **ADS**, **APrS**, and **APS** (see Table 1). The maximum current efficiency of **ANS** was lowest at 0.03 cd/A.

The EL  $\lambda_{\text{max}}$  values of all the doped devices are in the region of 450–470 nm, with the observed red shift in the devices doped with sulfur-containing materials. The non-doped device emitted purple-

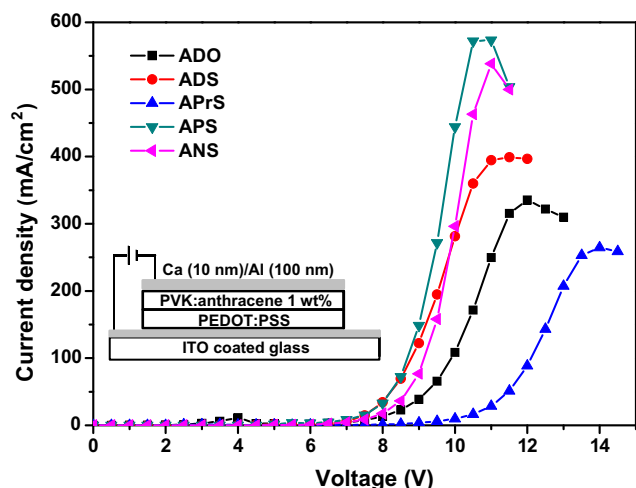


**Figure 3.** The current density versus voltage plots of the anthracene derivative doped devices.

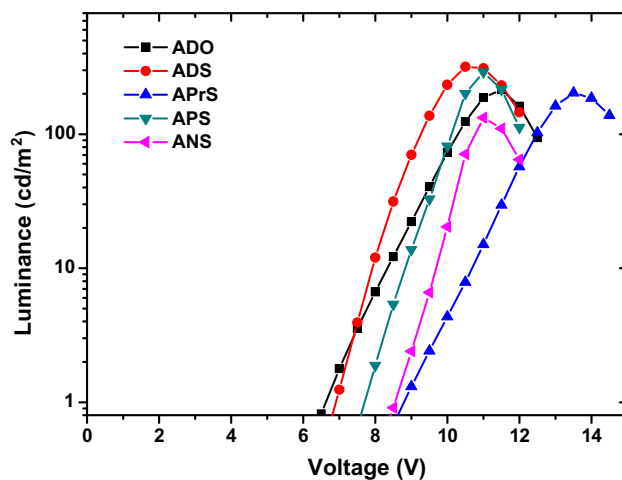


**Figure 4.** The luminance versus voltage plots of the anthracene derivative doped devices.

blue light with a peak at 440 nm, from the luminescence of PVK, corresponding to the CIE coordinates of (0.25, 0.20). In the presence of the doped material, the EL  $\lambda_{\text{max}}$  of the device is red shifted (Fig. 6): **ADO** 450 nm, CIE (0.17, 0.14), **ADS** 465 nm, CIE (0.16, 0.16), **APrS** 465 nm, CIE (0.17, 0.17), **APS** 465 nm, (0.17, 0.18) and **ANS** 470 nm, CIE (0.20, 0.22), indicating energy transfer from PVK to

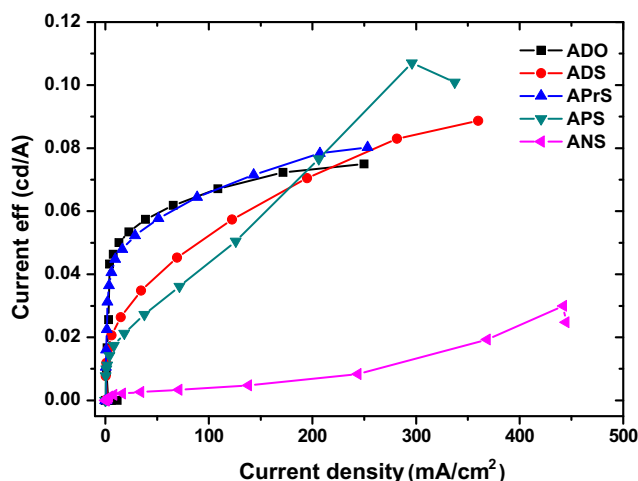


**Figure 5.** Current efficiency versus current density of anthracene derivative based devices.

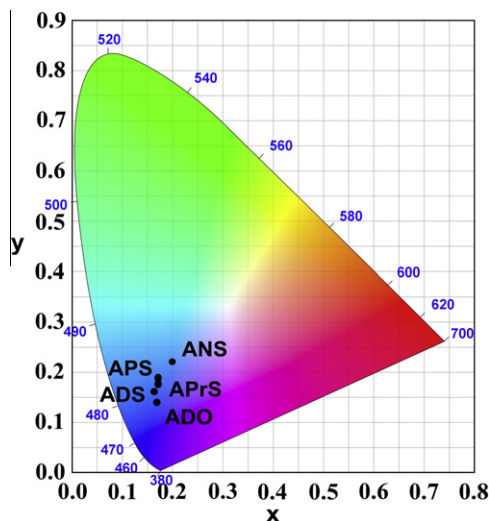


**Figure 6.** The Commission Internationale de L'Eclairage (CIE) chromaticity coordinates of the doped devices.

the anthracene derivatives. Moreover, the results showed that the length of the alkyl side chain has only a small effect on the luminescence properties of the molecules, while the effect of the aryl side chain was more drastic.

In conclusion, incorporation of chalcogen atoms, especially sulfur, onto the anthracene core drastically changes the photo and electronic properties of the molecules. This work has demonstrated the potential application of this new class of sulfur-containing materials for OLED devices. Further research on the design of more efficient sulfur-containing dopants as well as the device fabrication technique is required to improve the EL efficiency and these studies are currently in progress.

## 2. Typical procedure for the synthesis of anthracene bisulfide derivatives

### 2.1. 9,10-Bis(1-dodecylthio)anthracene (ADS)

A mixture of 9,10-diacetoxyanthracene (0.74 g, 2.51 mmol) and 1-dodecanethiol (6.03 g, 25.1 mmol) was refluxed in toluene (20.0 mL) in the presence of *p*-toluenesulfonic acid (4.78 g, 25.1 mmol) for 6 h. The reaction was cooled to room temperature and quenched with sat.  $\text{NaHCO}_3$  (20 mL) and then extracted with EtOAc ( $3 \times 30$  mL). The combined organic extract was washed with  $\text{H}_2\text{O}$ , dried over  $\text{Na}_2\text{SO}_4$  and evaporated to dryness. The crude product was purified by crystallization from a solution of  $\text{CH}_2\text{Cl}_2/\text{MeOH}$

to yield 9,10-bis(1-dodecylthio)anthracene (ADS) (1.18 g, 81% yield).

## Acknowledgments

Financial support from the National Synchrotron Research Center (Grant 2-2549/PSO1) for T.T. and scholarship support from the Royal Golden Jubilee (RGJ) program, the Development and Promotion of Science and Technology Talents (DPST) and the Center for Innovation in Chemistry: Postgraduate Education and Research Program in Chemistry (PERCH-CIC) for C.N., P.W., and K.S. are gratefully acknowledged.

## Supplementary data

Supplementary data (the synthesis,  $^1\text{H}$  and  $^{13}\text{C}$  NMR spectra and cyclic voltammograms (CV) of compounds ADO, ADS, APrS, APS and ANS) associated with this article can be found, in the online version, at doi:10.1016/j.tetlet.2010.09.089.

## References and notes

- For some selected examples, see: (a) Yeh, H.-C.; Chan, L.-H.; Wu, W.-C.; Chen, C.-T. *J. Mater. Chem.* **2004**, *14*, 1293; (b) Chen, C. H.; Tang, C. W.; Shi, J.; Klubek, K. P. *Thin Solid Films* **2000**, *363*, 327; (c) Thomas, K. R. J.; Lin, J. T.; Tao, Y.-T.; Chuen, C.-H. *Adv. Mater.* **2002**, *14*, 822; (d) Ma, C.-Q.; Liang, Z.; Wang, X.-S.; Zhang, B.-W.; Cao, Y.; Wang, L.-D.; Qiu, Y. *Synth. Met.* **2003**, *138*, 537.
- For selected examples, see: (a) Lee, M.-T.; Yen, C.-K.; Yang, W.-P.; Chen, H.-H.; Liao, C.-H.; Tsai, C.-H.; Chen, C. H. *Org. Lett.* **2004**, *6*, 1241; (b) Yu, M.-X.; Duan, J.-P.; Lin, C.-H.; Cheng, C.-H.; Tao, Y.-T. *Chem. Mater.* **2002**, *14*, 3958; (c) Chen, C. H.; Tang, C. W. *Appl. Phys. Lett.* **2001**, *79*, 3711; (d) Tao, Y. T.; Balasubramaniam, E.; Danel, A.; Jarosz, B.; Tomasik, P. *Appl. Phys. Lett.* **2000**, *77*, 1575.
- For some selected examples, see: (a) Mitsumori, T.; Bendikov, M.; Dautel, O.; Wudl, F.; Shioya, T.; Sato, H.; Sato, Y. *J. Am. Chem. Soc.* **2004**, *126*, 16793; (b) Wu, Y. Z.; Zheng, X. Y.; Zhu, W. Q.; Sun, R. G.; Jiang, X. Y.; Zhang, Z. L.; Xu, S. H. *Appl. Phys. Lett.* **2003**, *83*, 5077; (c) Lee, M.-T.; Liao, C.-H.; Tsai, C.-H.; Chen, C. H. *Adv. Mater.* **2005**, *17*, 2493.
- (a) Tao, S.; Xu, S.; Zhang, X. *Chem. Phys. Lett.* **2006**, *429*, 622; (b) Zhang, Z.; Tang, H.; Wang, H.; Liang, X.; Lui, J.; Qiu, Y.; Shi, G. *Thin Solid Films* **2007**, *515*, 3893; (c) Shen, W.-J.; Dodda, R.; Wu, C.-C.; Wu, F.-I.; Lui, T.-H.; Chen, H.-H.; Chen, C. H.; Shu, C.-F. *Chem. Mater.* **2004**, *16*, 930; (d) Danel, K.; Huang, T.-H.; Lin, J. T.; Tao, Y.-T.; Chuen, C.-H. *Chem. Mater.* **2002**, *14*, 3860; (e) Gebeyehu, D.; Walzer, K.; He, G.; Pfeiffer, M.; Leo, K.; Brandt, J.; Gerhard, A.; Stöbel, P.; Vestweber, H. *Synth. Met.* **2005**, *148*, 205.
- Kobayashi, K.; Masu, H.; Shuto, A.; Yamaguchi, K. *Chem. Mater.* **2005**, *17*, 6666.
- Kraus, G. A.; Man, T. O. *Synth. Commun.* **1986**, *16*, 1037.
- Sadorn, K.; Sinananwanich, W.; Areephong, J.; Wongma, C.; Nerungsi, C.; Pakawatchai, C.; Thongpanchang, T. *Tetrahedron Lett.* **2008**, *49*, 4519.
- Charoonniyomporn, P.; Thongpanchang, T.; Witayakarn, S.; Thebtaranonth, Y.; Phillips, K. E. S.; Katz, T. J. *Tetrahedron Lett.* **2004**, *45*, 457.
- Pardo, A.; Reyman, D.; Poyato, J. M. L.; Medina, F. *J. Lumin.* **1992**, *51*, 269.
- Beecroft, R. A.; Davidson, R. S.; Goodwin, D.; Pratt, J. E. *Tetrahedron* **1984**, *40*, 4487.
- Sasaki, H.; Wakayama, Y.; Chikyow, T.; Barrera, E.; Dosch, H.; Kobayashi, K. *Appl. Phys. Lett.* **2006**, *88*, 081907.
- Zhang, Y.; Hu, Y.; Chen, J.; Zhou, Q.; Ma, D. *J. Phys. D: Appl. Phys.* **2003**, *36*, 2006.